

LETTER • OPEN ACCESS

Impacts of rising air temperatures on electric transmission ampacity and peak electricity load in the United States

To cite this article: Matthew Bartos *et al* 2016 *Environ. Res. Lett.* **11** 114008

View the [article online](#) for updates and enhancements.

You may also like

- [Study of Temperature Field and Ampacity of 110kV AC Submarine Cables under Different Laying Conditions](#)
Zhenxin Chen, Yanjie Le, Heng Liu et al.
- [Section Selection Software Design for Submarine Cables](#)
Meng Li, Sheng-suo Niu, Yan Song et al.
- [Research on Optimum Laying Method for Increasing Underground Power Cable Ampacity](#)
Dan Pang, Haipeng Wu, Bin Dai et al.



The Breath Biopsy® Guide
Fourth edition

FREE

DOWNLOAD THE FREE E-BOOK

BREATH BIOPSY

OWLSTONE MEDICAL

Environmental Research Letters



LETTER

OPEN ACCESS

RECEIVED

31 December 2015

REVISED

26 September 2016

ACCEPTED FOR PUBLICATION

14 October 2016

PUBLISHED

2 November 2016

Original content from this work may be used under the terms of the [Creative Commons Attribution 3.0 licence](#).

Any further distribution of this work must maintain attribution to the author(s) and the title of the work, journal citation and DOI.



Impacts of rising air temperatures on electric transmission ampacity and peak electricity load in the United States

Matthew Bartos^{1,4}, Mikhail Chester¹, Nathan Johnson², Brandon Gorman¹, Daniel Eisenberg^{1,3}, Igor Linkov³ and Matthew Bates³

¹ Department of Civil, Environmental and Sustainable Engineering, Arizona State University, USA

² The Polytechnic School, Ira A. Fulton Schools of Engineering, Arizona State University, USA

³ US Army Engineer Research and Development Center, Vicksburg, MS, USA

⁴ Author to whom any correspondence should be addressed.

E-mail: mdbartos@umich.edu, mchester@asu.edu, nathanjohnson@asu.edu, btgorman@asu.edu, daeisenb@asu.edu, igor.linkov@usace.army.mil and matthew.e.bates@usace.army.mil

Keywords: climate change, infrastructure, resilience, electrical grid

Supplementary material for this article is available [online](#)

Abstract

Climate change may constrain future electricity supply adequacy by reducing electric transmission capacity and increasing electricity demand. The carrying capacity of electric power cables decreases as ambient air temperatures rise; similarly, during the summer peak period, electricity loads typically increase with hotter air temperatures due to increased air conditioning usage. As atmospheric carbon concentrations increase, higher ambient air temperatures may strain power infrastructure by simultaneously reducing transmission capacity and increasing peak electricity load. We estimate the impacts of rising ambient air temperatures on electric transmission ampacity and peak per-capita electricity load for 121 planning areas in the United States using downscaled global climate model projections. Together, these planning areas account for roughly 80% of current peak summertime load. We estimate climate-attributable capacity reductions to transmission lines by constructing thermal models of representative conductors, then forcing these models with future temperature projections to determine the percent change in rated ampacity. Next, we assess the impact of climate change on electricity load by using historical relationships between ambient temperature and utility-scale summertime peak load to estimate the extent to which climate change will incur additional peak load increases. We find that by mid-century (2040–2060), increases in ambient air temperature may reduce average summertime transmission capacity by 1.9%–5.8% relative to the 1990–2010 reference period. At the same time, peak per-capita summertime loads may rise by 4.2%–15% on average due to increases in ambient air temperature. In the absence of energy efficiency gains, demand-side management programs and transmission infrastructure upgrades, these load increases have the potential to upset current assumptions about future electricity supply adequacy.

Glossary

| | |
|-------------|--|
| \dot{q}_c | Convective heat loss from conductor to air (W m^{-1}) |
| \dot{q}_r | Radiative heat loss from conductor to surroundings (W m^{-1}) |

 \dot{q}_s

Radiative heat transfer from sun to conductor (W m^{-1})

 \dot{q}_j

Resistive heating of the conductor (W m^{-1})

 I

Conductor current (A)

| | |
|-------------------|---|
| T_{cond} | Average conductor temperature (K) |
| R | AC resistance of conductor ($\Omega \text{ m}^{-1}$) |
| \bar{h} | Average heat transfer coefficient ($\text{W m}^{-2} \text{ K}^{-1}$) |
| D | Conductor diameter (m) |
| T_{amb} | Ambient air temperature (K) |
| T_f | Film temperature (K) |
| ε | Emissivity of conductor surface (dimensionless) |
| σ | Stefan–Boltzmann constant ($5.670\text{e-}8 \text{ W m}^{-2} \text{ K}^{-4}$) |
| δ | Incident solar radiation (W m^{-2}) |
| a_s | Absorptivity of conductor surface (dimensionless) |
| d | Per-capita electricity load (W per capita) |

1. Introduction

Climate change may adversely affect electricity supply adequacy by reducing generation and transmission capacity while simultaneously increasing electricity demand. Extreme heat and drought can impair power generation capacity [1–3], limit the current-carrying capacity (ampacity) of transmission lines [3], and increase peak electricity loads [3, 4]. As atmospheric carbon concentrations increase, extreme heat and drought events are expected to occur with greater frequency, meaning that power infrastructure may be placed under greater strain for longer periods of time [5]. Future drought conditions have the potential to limit power generation at ‘base-load’ power plants—which require a consistent supply of water for cooling [1, 2, 6–9]. Similarly, extreme heat may reduce the power output of peaking generation sources like gas turbines, which become less efficient as the density of air decreases [1, 3], and photovoltaic solar cells, which lose efficiency at high air temperatures due to increased carrier recombination rates [10]. By mid-century, changes in climate may reduce vulnerable generation capacity in the Western US by as much as 1.1%–3.0% in an average year, and up to 7.2%–8.8% under a ten-year drought scenario [1]. Although these capacity reductions are significant in their own right, impacts to power generation are likely to occur alongside impacts to electricity transmission and demand. Elevated air temperatures can reduce the rated capacity of electric transmission lines, meaning that their ability to transmit power will be diminished during peak hours. Higher temperatures may also increase electricity loads for air conditioning during the summer period,

and although only one-half of United States utilities experience peak summer load in the summer, the aggregation of these utilities create a nationwide peak load that is higher in the summer than in other parts of the year, thereby indicating summer as the period of interest when considering nationwide transmission infrastructure vulnerability to rising ambient air temperatures [11, 12]. The opposite effect may be observed in other periods of the year with different energy use patterns, such as colder regions with electric resistance heating or electric heat pumps in buildings that create an annual peak load in the winter rather than the summer [13], and this peak may be reduced as ambient temperatures increase in winter [12]. Nevertheless, for the summer period, rises in ambient temperature create coincident impacts to electricity generation, transmission and peak load that may result in a more vulnerable electric grid in certain regions of the US. Traditionally, risk analysis for electric power systems has taken the form of probabilistic methods based on historical conditions [14]. In a future characterized by changing climatic conditions, increased grid complexity, and augmented operational ‘interconnectedness’, this approach may no longer be sufficient to protect against outages and other grid disruptions [14, 15]. Failure to account for the effects of climate change on the electrical grid may leave regional planning authorities unprepared for future electricity shortages.

The effects of climate change on overall electric power reliability have yet to be fully explored. It is, however, possible that rising electrical loads combined with a reduction in electrical generation and/or line carrying capacity will narrow the band of operational stability and safety. Broadly, electricity supply adequacy can be described as a function of three factors: (1) achievable generation capacity, (2) transmission and distribution capacity, and (3) expected peak load. While previous research has assessed climate impacts to each of these components in isolation, it has so far proven difficult to assess how the combined impacts to generation, transmission and peak load may affect overall electricity supply adequacy. Evaluation of future electricity supply adequacy is complicated by a host of factors, including climate non-stationarity, system redundancy, power system regulations and industry norms. However, a major obstacle to evaluation of future electricity supply adequacy is the fact that impacts to generation, transmission and demand have been evaluated at varying local and regional scales, but have not been evaluated at the scale necessary for grid-level assessment. Several studies have assessed the potential impacts of climate change on power generation at national, interconnection and sub-interconnection scales [1–3]. However, transmission ampacity and peak electricity load also play an important role in determining a region’s overall electricity supply adequacy. Although the effects of ambient temperature on electric transmission capacity have long been recognized, power providers typically rate

system ampacity using historical temperature profiles [16, 17]. Sathaye *et al* [3] use global climate model (GCM) output to characterize the effects of climate change on transmission infrastructure in California, and find that transmission capacity may be reduced by 7%–8% by the end of the twenty-first century [3]. However, to our knowledge there is no study that estimates the impacts of rising temperatures on transmission capacity nationwide.

Several recent studies have assessed the potential impacts of climate change on energy consumption. However, these studies generally fall short of forecasting potential effects to electricity supply adequacy for a number of reasons: (1) they concentrate on increases to annual building energy consumption (i.e. MWh), as opposed to instantaneous peak load (i.e. MW), (2) they use a spatial extent or resolution that is not scalable to an interconnection-level assessment, or (3) they use assumed temperature increases, as opposed to spatially explicit GCM projections. Almost all previous studies focus on climate impacts to annual building energy consumption instead of peak electricity load [4]. Several studies assess changes to annual building energy demand at the national scale [18–23]; others focus on a particular region [24], using finer-scale temperature and infrastructure data [24]. While these studies help to predict the increased primary energy burden resulting from climate change, they do not indicate how climate change will affect the capacity needed during peak times. Franco and Sanstad [25] and Sathaye *et al* [3] estimate climate impacts to peak load in California. However, in terms of electrical infrastructure, California is not an isolated system, and relies on interstate electricity transfers to meet demand [26]. Thus, impacts to California's peak period infrastructure do not necessarily reflect overall electricity supply adequacy at the interconnection scale. Reference [27] investigate spatially explicit changes in electricity load at the neighborhood scale using high-resolution downscaled climate model output in the Southeastern United States. Dirks *et al* [4] use a highly detailed building energy model to assess climate effects on peak electricity load in the Eastern Interconnection using one climate model scenario [4]. However, to our knowledge there has been no comprehensive, national-scale assessment of peak load impacts under a range of possible climate change scenarios. Because of the relative lack of research on peak demand and transmission impacts at the interconnection scale, there remain significant unknowns as to the effects of climate change on electricity reliability. To address these knowledge gaps, we estimate impacts to electricity transmission capacity and summertime peak per-capita load over the continental United States.

2. Methodology

We estimate the impacts of climate change on (a) the rated ampacity of transmission lines and (b) expected summertime peak per-capita electricity load for 121 electric service planning areas across the US. Together, these planning areas supply roughly 650 GW of power [28]—about 80% of current peak summertime load in the US [29]. Our analysis takes place in two parts. In the first phase, we estimate climate-attributable capacity reductions to aerial transmission lines by constructing thermal models of representative conductors and forcing these models with temperature projections (from 2010–2100) to determine the relative change in safe operating ampacity. In the second phase, we characterize climate impacts on electricity load by using historical relationships between ambient temperature and summertime per-capita peak load to estimate the extent to which climate change may incur additional load increases. To account for variability in GCM projections, we use output from 11 different GCM models with 2–3 representative concentration pathway (RCP) scenarios per model. After estimating climate-attributable impacts to both electricity transmission and load, we discuss how atmospheric carbon reductions, heat-resistant conductors and smart-grid technologies can mitigate the effects of rising air temperatures on electricity peak-period infrastructure.

2.1. Estimating climate impacts to electric transmission capacity

We estimate the impacts of climate change on electric transmission capacity by developing thermal models of representative electric transmission cables, then forcing these models with downscaled temperature projections over the period 2010–2100. Electric power cables suffer decreased transmission capacity as the temperature of the conductor increases [30]. A portion of these capacity losses result from increased electrical resistance at higher conductor temperatures [30]. However, the current-carrying capacity of a transmission line is primarily limited by a conductor's maximum allowed operating temperature [30]. Maximum operating temperatures are prescribed for different types of conductors to (a) ensure compliance with clearance regulations, and (b) prevent damage to the conductor and other line hardware [16]. For a typical aluminum conductor steel-reinforced cable, allowable temperatures may range from 50 °C to 180 °C depending on the duration of heat exposure, and engineering practice and judgment [30]. Continued operation beyond a conductor's maximum operating temperature can result in excessive sag or damage [30]. To avoid surpassing a transmission line's maximum operating temperature, operators typically curtail the current in an at-risk conductor such that thermal

limits are satisfied [3, 30]. Thus, electric power cables are generally given a ‘rated ampacity’, which represents the maximum current for which conductor temperature limits are met under standard ambient temperature and wind conditions [3, 30]. Hotter air temperatures due to anthropogenic global warming may reduce the effective ampacity of transmission lines by interfering with their ability to dissipate heat [30]. To gauge potential ampacity reductions under changing climatic conditions, we develop a thermal balance model to estimate the rated ampacity of transmission lines based on cable properties and meteorological forcings. We then force this thermal balance model with future temperature projections to determine the percent change in rated ampacity for transmission lines in the US.

We simulate the rated ampacity of power lines using an energy balance approach

$$\Delta \dot{E} = \dot{q}_j + \dot{q}_s - \dot{q}_c + \dot{q}_d - \dot{q}_r. \quad (1)$$

Assuming steady-state conditions ($\Delta \dot{E} = 0$) and no conduction ($\dot{q}_d = 0$), the energy balance of a conductor can be resolved into four heat transfer components: (1) heat gain from the electrical current flowing through the conductor, \dot{q}_j , (2) heat gain from solar radiation striking the top half of the surface of the conductor, \dot{q}_s , (3) heat loss due to convection, \dot{q}_c , and (4) heat loss due to radiation, \dot{q}_r [30]. To satisfy equilibrium conditions, the total heat transfer into the conductor must equal the total heat transfer out of the conductor

$$\dot{q}_c + \dot{q}_r = \dot{q}_s + \dot{q}_j. \quad (2)$$

Heat gain due to electrical loading (known as Joule heating) is a function of the current transferred through the conductor (I) and the resistance of the conductor at a given conductor temperature, $R(T_{\text{cond}})$ [30]

$$\dot{q}_j = I^2 \cdot R(T_{\text{cond}}). \quad (3)$$

Rearranging the heat balance yields the maximum allowable current (the rated ampacity) as the dependent variable

$$I = \sqrt{\frac{\dot{q}_c + \dot{q}_r - \dot{q}_s}{R(T_{\text{cond}})}}. \quad (4)$$

In expanded form, the rated ampacity of an overhead conductor can be expressed in terms of ambient weather conditions (temperature and wind speed), solar insolation, and cable properties (diameter, surface area and material properties). For a full derivation, see section 1.1.1 in the supplementary information (SI) document

where \bar{h} is the average heat transfer coefficient, D is the cable diameter, T_{amb} is the ambient air temperature, ε is the emissivity of the conductor surface, σ is the Stefan–Boltzmann constant, δ is the incident solar radiation, and a_s is the absorptivity of conductor surface.

We apply the thermal balance model to existing and proposed transmission lines in the United States to predict the relative decrease in rated ampacity under future climatic conditions. We use the Homeland Security Infrastructure Program (HSIP) database to determine the locations, geometries and voltage classes for both existing and proposed transmission lines [31]. This dataset includes 50 822 existing and 1184 proposed high-voltage transmission lines throughout the continental US. Representative model cables are generated for each standard voltage class (69, 138, 230, 345 and 525 kV) based on reported conductor specifications (see SI section 1.1.3). Manufacturer data are used to determine relevant design specifications for model cables, such as conductor diameter and AC resistance [32–34]. We use a maximum allowable conductor temperature of 75 °C, a representative wind speed of 0.61 m s^{−1} perpendicular to the conductor axis, and a solar insolation intensity of 1000 W m^{−2} to represent full sun conditions, per standard ampacity calculation protocols used by manufacturers to rate the ampacity of aluminum-conductor steel-reinforced (ACSR) conductors (the most common conductor type currently in use) [32–35]. Although average solar insolation varies by geographical location, we use a fixed solar insolation value of 1000 W m^{−2} to (i) evaluate ampacity under ‘worst-case’ (full sun) conditions, and (ii) to maintain consistency with existing ampacity rating protocols. We do not model long-term changes in wind speed, given that wind speed in the continental US is not expected to change significantly as a result of climate change (see SI section 2.5), though it should be noted that the effect of climate change on continental wind speed is still a debated subject. For our base-case scenario, we assume that the conductor technologies used for proposed cables will be similar to those used for existing cables. However, adoption of more heat-resistant conductor technologies—such as aluminum conductor steel supported (ACSS) conductors—can help to mitigate impacts posed by rising air temperatures. The effect of using more heat-resistant conductors is explored in SI section 2.3. Other assumed parameters used in the thermal model (including emissivity and absorptivity) can be found in SI table S3.

The thermal balance model is executed at a daily time step (using daily maximum temperature) to

$$I = \sqrt{\frac{\pi \cdot \bar{h} \cdot D \cdot (T_{\text{cond}} - T_{\text{amb}}) + \pi \cdot \varepsilon \cdot \sigma \cdot D \cdot (T_{\text{cond}}^4 - T_{\text{amb}}^4) - \delta \cdot D \cdot a_s}{R(T_{\text{cond}})}} \quad (5)$$

Table 1. Global climate models selected from the Coupled Model Intercomparison Project Phase 5 (CMIP5) multi-model ensemble for use in this study. The modeling group responsible for each GCM model is shown on the leftmost column, while the representative concentration pathway (RCP) scenarios included are shown in the rightmost column. The r1i1p1 ensemble member is used for all GCM models.

| Modeling group | GCM model | RCP scenarios included |
|---|---------------|------------------------|
| Canadian Centre for Climate Modelling and Analysis | CanESM2 | 2.6, 4.5, 8.5 |
| National Center for Atmospheric Research | CCSM4 | 2.6, 4.5, 8.5 |
| Community Earth System Model Contributors | CESM1-BGC | 4.5, 8.5 |
| Centre National de Recherches Météorologiques / Centre Européen de Recherche et Formation Avancée en Calcul Scientifique | CNRM-CM5 | 4.5, 8.5 |
| Commonwealth Scientific and Industrial Research Organization in collaboration with Queensland Climate Change Centre of Excellence | CSIRO-Mk3.6.0 | 2.6, 4.5, 8.5 |
| NOAA Geophysical Fluid Dynamics Laboratory | GFDL-ESM2G | 2.6, 4.5, 8.5 |
| NOAA Geophysical Fluid Dynamics Laboratory | GFDL-ESM2M | 2.6, 4.5, 8.5 |
| Institut Pierre-Simon Laplace | IPSL-CM5A-MR | 2.6, 4.5, 8.5 |
| Atmosphere and Ocean Research Institute (The University of Tokyo), National Institute for Environmental Studies, and Japan Agency for Marine-Earth Science and Technology | MIROC5 | 2.6, 4.5, 8.5 |
| Max Planck Institute for Meteorology | MPI-ESM-LR | 2.6, 4.5, 8.5 |
| Max Planck Institute for Meteorology | MPI-ESM-MR | 2.6, 4.5, 8.5 |

determine the reduction in rated ampacity between historical and future scenarios. For the historical period, we force the thermal model with gridded observed daily maximum temperature data from 1990–2010 [36]. The temperature forcings included in this dataset are derived from National Oceanic and Atmospheric Administration (NOAA) Cooperative Observer stations, which are gridded to a spatial resolution of 1/8 degree (roughly 12 km) using the synergraphic mapping system (SYMAP) algorithm [37, 38]. For the future period, we use downscaled daily maximum temperature data from the Coupled Model Intercomparison Project Phase 5 (CMIP5) multi-model ensemble of GCMs [39]. CMIP5 is the latest iteration of the CMIP project, which aims to cultivate a standardized protocol for comparing outputs of coupled atmosphere-ocean general circulation models. Projected temperature data from GCMs are gridded at a spatial resolution of 1/8 degree using the bias-corrected constructed analogue downscaling method. Temperature data are joined to each transmission cable in the HSIP dataset based on spatial location. To capture a range of possible futures, we use the RCP 2.6, 4.5 and 8.5 RCPs proposed by the Intergovernmental Panel on Climate Change. These scenarios prescribe anticipated ranges of anthropogenic warming based on divergent trends in atmospheric carbon concentrations, and provide a basis for measuring the impacts of climate change under different social, technical and policy scenarios. The specific GCMs and RCP scenarios used in this study are shown in table 1.

2.2. Estimating peak per-capita load increases due to elevated air temperatures

Climate change may strain power infrastructure by increasing loads during the summer peak period. During the summer months, electricity load typically increases with hotter air temperatures due to increased air-conditioning usage [3, 40]. Across the continental

US, average daily maximum summertime temperatures are expected to increase by as much as 1 °C–5 °C by mid-century [39]. In the absence of building energy efficiency gains and load management programs, these higher temperatures are likely to result in higher per-capita electricity loads for summer-peaking regions, where air conditioning use is closely tied to ambient air temperature. We model potential increases to peak per-capita summertime electricity load for 121 unique planning areas (comprising 1044 individual retail electric service providers) in the United States based on historical relationships between air temperature and load. These planning areas account for about 650 GW of summertime load (or about 80% of peak summertime load in the United States). To estimate potential per-capita load increases under future climate scenarios, we first develop regression relationships between peak daily per-capita load and maximum daily temperature using historical population, load and temperature data. Next, we force these regression models with projected temperature data from the CMIP5 multi-model GCM ensemble.

Because average annual electricity load scales with population [3], it is necessary to remove the effect of population growth before a relationship between temperature and peak load can be observed. To this end, we estimate peak per-capita electricity load for planning areas using reported hourly loads along with population estimates from the US Census. Hourly loads from 1993–2010 are determined for major electrical planning areas using Federal Energy Regulatory Commission (FERC) Form 714 [41]. Next, population estimates are generated for each planning area using census tract-level population estimates for the years 1990, 2000 and 2010 [42–44]. Census tracts are spatially joined to the planning areas that intersect them. We use census tract boundary files from the US Census Bureau's Topologically Integrated Geographic Encoding and Referencing (TIGER/Line) database

[45–47], and retail electric service area boundaries from the HSIP GIS database [28], which are aggregated into their respective planning areas. The population in each planning area is taken as the sum of the census tract populations that intersect that planning area. Per capita electricity load is then computed for each planning area for the period 1993–2010 by combining population and hourly load data developed in the previous steps. It should be noted that socio-economic factors—such as gross domestic product, household income, and electricity prices—can also influence electricity load [48–50]. When predicting total electricity load under future scenarios (particularly over a short time horizon), it is sometimes necessary to take these factors into account. In this study, we do not account for changes in socio-economic indicators for two primary reasons: (1) these socio-economic indicators cannot be meaningfully projected over the 35–85 year time horizon used in this paper, and (2) we are interested primarily in isolating the marginal increase in per-capita electricity load due to long-term changes in air temperature, rather than absolute future electricity load. In this formulation, socio-economic factors appear as part of the variance in the temperature-load response function. Similarly, technological changes—such as improved building energy efficiency or market saturation of air conditioning units—can also affect the temperature-load response function. Rising temperatures may, for instance, promote the adoption of air conditioning units in regions where their usage was historically more limited [51]. We acknowledge that changes beyond what we estimate in our model are possible, and discuss these sources of uncertainty in greater detail in section 4.

Having estimated per-capita load for major planning areas in the US, historical temperature data are used to construct temperature-load regression equations, which are then forced with projected temperature data to determine the expected changes in peak per-capita summertime load under future climatic conditions. Gridded historical daily maximum temperature data are first assigned to each planning area using a spatial join [36]. For planning areas with a single urban area, temperature data nearest to the centroid of the urban area are used. For planning areas that contain multiple urban areas, the process of rendering a representative temperature cell takes place in two steps: (1) gridded temperature data nearest to the centroid of each urban area are collected, and (2) a weighted average temperature for the entire planning area is generated, with the weights being determined by the populations of each urban area. After determining representative temperatures for each planning area for the period 1993–2010, regression relationships between daily maximum temperature and daily peak load are developed for the summer peak period (June–August). Regression relationships take the form of a quadratic equation, with ambient daily maximum temperature as the independent variable, and peak

per-capita electricity load as the dependent variable

$$d = \alpha \cdot T_{\text{amb}}^2 + \beta \cdot T_{\text{amb}} + \gamma, \quad (6)$$

where α , β and γ are empirically determined coefficients. A quadratic equation is selected for the regression model because it provides a good fit for most planning areas (with an average R^2 coefficient of 0.6 over the 121 planning areas considered), and because higher-order models can result in very large loads when extrapolated beyond the historical temperature range (SI section 2.4). Planning areas with an R^2 coefficient below 0.5 are not included in the results. It should be noted that although this study develops a regression relationship between ambient temperature and total per-capita load, not all of electricity load is sensitive to changes in air temperature. The regression relationships developed for each planning area are forced with downscaled CMIP5 GCM projections of daily maximum temperature to determine the increase in summertime peak per-capita load over the 21st century [39].

3. Results

By mid-century (2040–2060), rising air temperatures may reduce summertime transmission capacity by 1.9%–5.8% on average, relative to the 1990–2010 reference period (with the range of impacts being dependent on GCM model and RCP scenario selection). These reductions in rated ampacity may pose challenges for transmission planning authorities, who typically design peak period infrastructure based on historical conditions. Figure 1 shows maps of expected ampacity reductions by decade under the ‘medium’ atmospheric carbon concentration scenario (RCP 4.5). Impacts to transmission capacity vary with both geographic location and conductor technology. Ampacity reductions are typically largest in the FERC Midcontinent (MISO) electricity market, where average summertime daily maximum temperatures are likely to rise by as much as 2 °C–5 °C. By contrast, transmission lines experience smaller ampacity reductions along the coastal regions, where temperature increases are more moderate. Although impacts vary by geographic region, almost all transmission lines in the US are expected to experience ampacity reductions. In addition to geographic location, conductor properties also play a role in determining expected climatic impacts to transmission capacity. In general, high-voltage lines suffer greater capacity reductions than lower-voltage lines. This is because high-voltage lines are generally thicker, making heat dissipation more difficult. While geographic and technological factors play a role in determining the vulnerability of transmission lines, reductions in rated ampacity are most sensitive to increases in ambient air temperature. Figure 2 shows histograms of percent reduction in rated ampacity by decade for three carbon

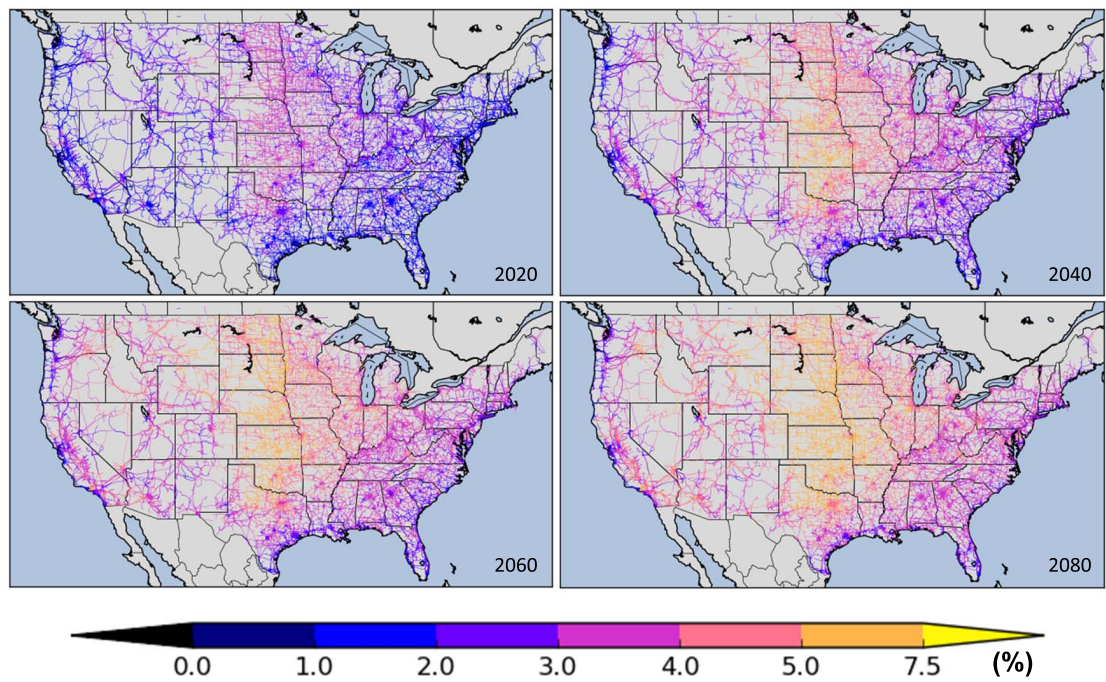


Figure 1. Climate attributable reductions to transmission capacity by decade (from top left to bottom right: 2020, 2040, 2060, 2080). Colors indicate the percent reduction in transmission capacity under the average RCP 4.5 scenario, relative to the 1990–2010 reference period. For additional information on transmission line visualizations, see SI section 4.6.

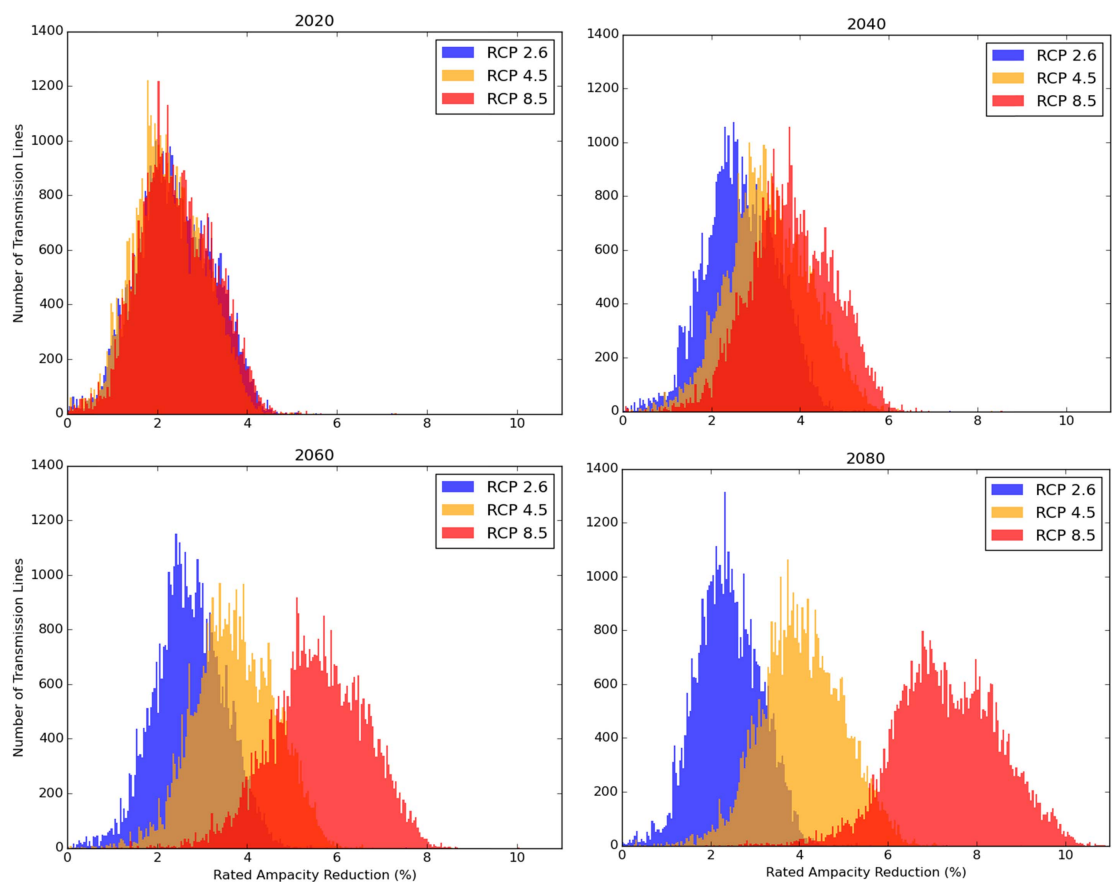
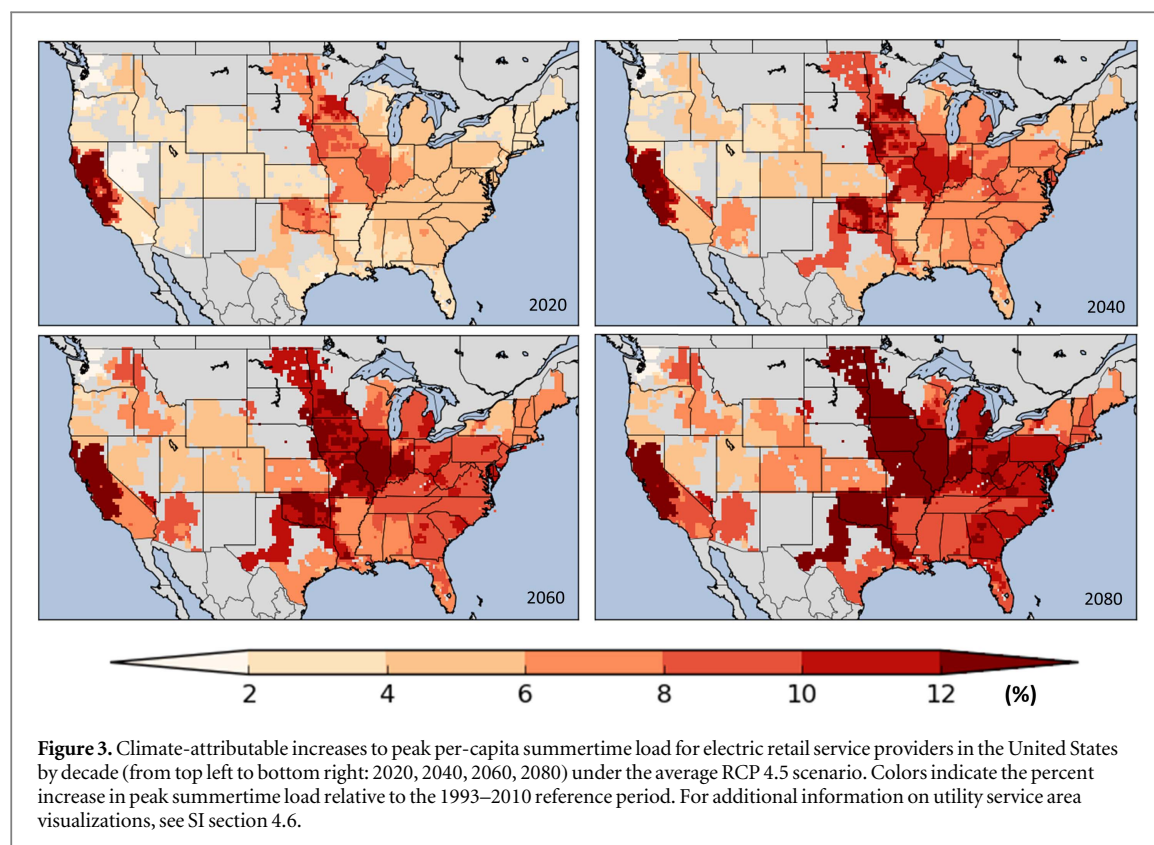


Figure 2. Histograms indicating percent reduction to transmission capacity by decade (from top left to bottom right: 2020, 2040, 2060, 2080). RCP scenarios (2.6, 4.5 and 8.5) are indicated by their respective colors (blue, yellow and red). The horizontal axis represents bins of percent ampacity reductions, while the vertical axis represents the number of transmission lines falling into each bin.



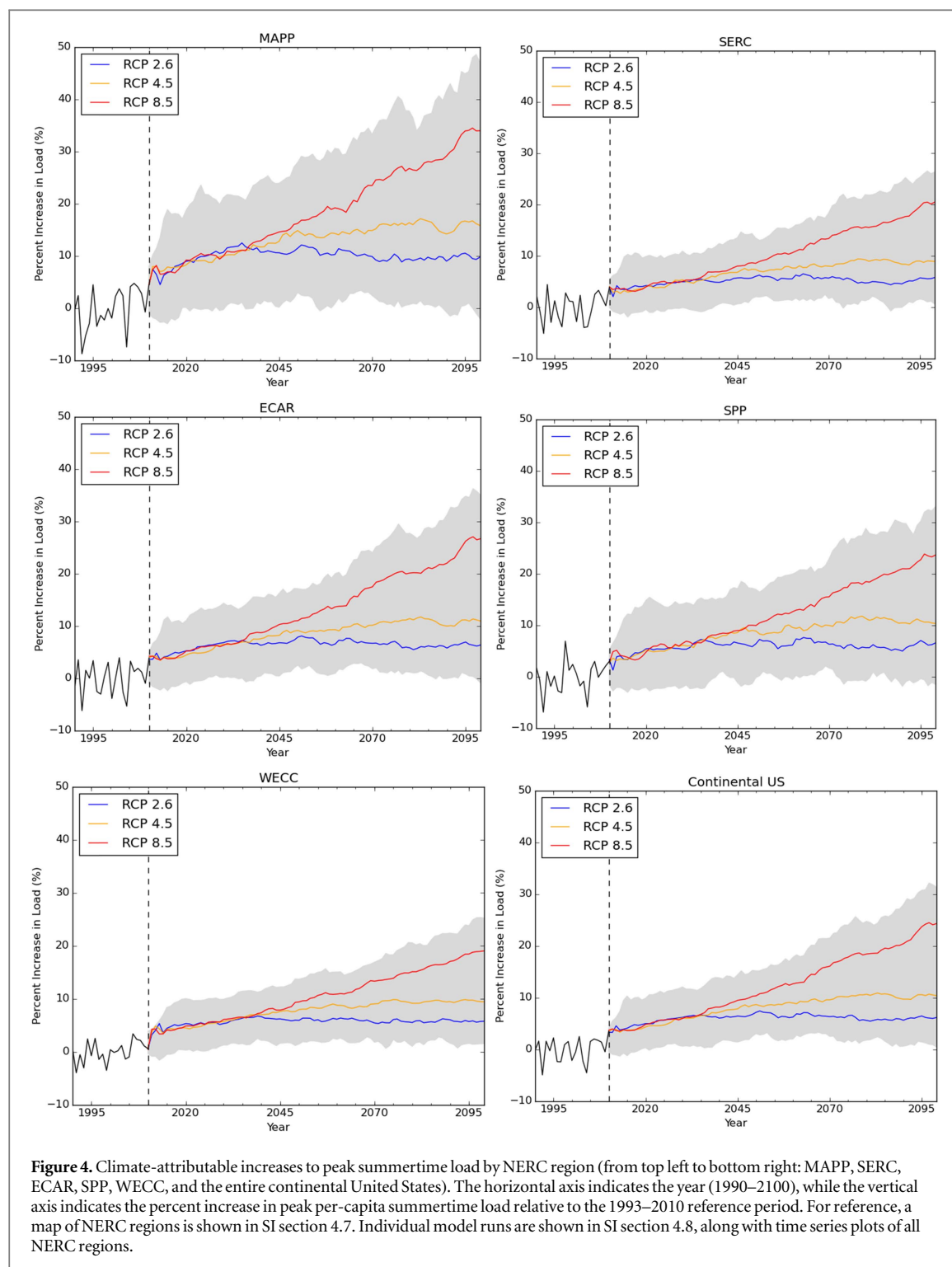
concentration scenarios—RCP 2.6, 4.5 and 8.5. By mid-century, average transmission capacity reductions range from 1.9%–3.9% under the lowest carbon concentration scenario (RCP 2.6) to 2.2%–4.3% under the medium carbon concentration scenario (RCP 4.5), to 3.6%–5.8% under the highest carbon concentration scenario (RCP 8.5). This outcome suggests that impacts to transmission ampacity can be mitigated by policy efforts to reduce atmospheric carbon concentrations.

Increases to peak per-capita electricity load present perhaps the greatest climate impact-related challenge to electricity supply adequacy. By mid-century, peak per-capita summertime loads may rise by 4.2%–15% on average due to increases in daily maximum air temperature (with GCM and RCP selection accounting for the range of variability). In the absence of energy efficiency gains and demand-side management programs, these load increases could narrow the band of safe operating conditions, indicating greater grid vulnerability and reduced reliability. Figure 3 presents maps of summertime peak per-capita load by decade under the RCP 4.5 scenario, while figure 4 displays time series data of summertime peak per-capita load for all RCP scenarios over the period 1990–2100. Impacts to peak load are strongly correlated with the degree of air temperature rise. For the lowest carbon concentration trajectory (RCP 2.6), increases to per capita load level out at roughly 4.2%–9.2% by mid-century, while under the highest carbon concentration scenario (RCP 8.5), per capita loads may be 7.9%–15%

higher by mid-century, and may rise to as much as 30% by 2100. As with impacts to transmission capacity, climate-attributable load increases vary by geographical location. However, unlike impacts to transmission capacity, peak load increases are not necessarily correlated with the degree of temperature rise. In general, urban areas show greater climate-attributable load increases than rural areas. Populous states with large metropolitan areas—such as California, Illinois, Texas and New York—show some of the largest load increases, while sparsely populated states—such as Wyoming, Utah and Nevada—show relatively small load increases, despite being located in regions that are expected to receive above-average warming. This effect could be attributed to greater penetration and density of air conditioning units in urban areas, where building proximity prevents passive cooling. While increases to peak load vary by atmospheric carbon concentration and geographic region, overall per capita peak load is expected to increase for all scenarios considered. These climate-attributable increases to peak load are currently not accounted for by many planning authorities, meaning that planned peak period infrastructure may not optimally meet future electricity needs.

4. Uncertainty assessment

Climate impacts to electricity supply adequacy may be influenced by several sources of uncertainty—including climate model variability, unknown conductor



specifications, and future technological changes. Although these sources of uncertainty may affect the degree to which climate change impairs electricity reliability, it is unlikely that a scenario will occur in which transmission capacity is not reduced, or in which per capita peak electricity load does not increase. Variability in GCM model output represents the largest source of uncertainty in this study. Between GCM models, median impacts to transmission capacity range from about 1.7% (GFDL-ESM2M, RCP 2.6) to 5.6% (CANESM2, RCP 8.5) by mid-century, while

increases to electricity load range from about 4.3% (GFDL-ESM2M, RCP 2.6) to almost 15% (CSIRO-Mk3-6-0, RCP 8.5). Note that although both transmission and load losses depend on the amount of temperature rise, upper-bound impacts occur under different GCM models. This result is explained by spatial variability in temperature rise between models: impacts to electricity load are dependent on temperature changes over major population centers (non-uniformly distributed), while high voltage transmission lines are more evenly distributed, meaning that

impacts to transmission are more reflective of overall continental temperature rise. Although impacts vary widely between GCM models, this variability does not affect the primary conclusions of the study: all models predict overall reductions to transmission capacity and overall increases to peak electricity load. To ensure that the predicted impacts are not an artifact of GCM model variability, we test for the significance of our results using a Wilcoxon rank-sum test (see SI section 2.1). Transmission capacity and per capita electricity load are both found to be significantly affected by changes in climate ($p < 0.001$) for all GCM models and RCP scenarios considered.

In addition to GCM model uncertainty, we also assess several secondary sources of uncertainty, including (1) choice of representative conductor cables, (2) choice of maximum allowable conductor temperature, (3) choice of temperature-load regression model, and (4) potential for future changes in wind speed. Conductor model choice has a relatively minor effect on climate-attributable ampacity reductions ($<1\%$), and is unlikely to affect the primary results of this study (see SI section 2.2). Maximum allowable conductor temperature, on the other hand, can significantly affect temperature-related ampacity reductions (see SI section 2.3). Under the most conservative maximum conductor temperature ($75\text{ }^{\circ}\text{C}$), ampacity reductions range from 1.9% – 5.8% by mid-century, while for a more permissive maximum conductor temperature ($100\text{ }^{\circ}\text{C}$), climate-attributable ampacity reductions are on the order of 1.1% – 3.4% . Ultimately, we select a maximum conductor temperature of $75\text{ }^{\circ}\text{C}$ for ACSR cable, because it is the industry standard for continuous operation under normal conditions [35]. However, it should be noted that some climate impacts to transmission capacity may be avoided by allowing transmission lines to run at higher temperatures, or by installing more heat-resistant cables (such as ACSS). Because ACSS conductors are designed to withstand temperatures of $250\text{ }^{\circ}\text{C}$ without loss of strength [52], the effect of ambient temperature rise on these cables is comparatively small. In addition to assessing uncertain conductor parameters, we also assess the sensitivity of results to different temperature-load regression models (see SI section 2.4). We investigate three regression models (linear, quadratic and cubic) and find that the choice of regression model can significantly influence climate-attributable increases to peak electricity load. Impacts are fairly similar under the linear and quadratic regression models: by mid-century, summertime peak load is expected to increase by about 4.2% – 13% under the linear regression model, and about 4.2% – 15% under the quadratic regression model. However, the cubic regression model predicts much higher impacts than the other regression models, with expected peak load increases of roughly 11% – 40% . This outcome follows from the fact that high-order polynomial models tend to predict large loads when extrapolated beyond the

historical temperature range. All models offer similar goodness of fit, with average R^2 values of 0.58 , 0.6 and 0.6 for the linear, quadratic and cubic models, respectively. However, the linear model shows bias at the upper and lower ends of the temperature spectrum, where the temperature-load response function tends to show nonlinear behavior. Ultimately, we select the quadratic regression model because (i) it offers a better goodness of fit than the linear model, (ii) it captures historical temperature-load profiles over the entire range of expected temperatures and (iii) it is less susceptible to extrapolation errors than the cubic model. Conductor ampacity is strongly dependent on wind speed, suggesting that future changes in wind speed could potentially influence anticipated ampacity reductions. However, based on an assessment of projected wind speeds in the CMIP3 multi-model ensemble, we find that wind speeds are not expected to change significantly as a result of climate change (SI section 2.5). It should be noted, however, that the effects of climate change on wind speed are a subject of debate, with various studies predicting global trends of increasing wind speed [53], global trends of decreasing wind speed [54], 1.4% – 4.5% reductions in wind speed throughout the US over the next hundred years [55], decreased wind speed throughout the Western US High Plains Region [56], no detectable changes in US wind speed over the next half-century [57], and small magnitude changes ($\pm 0.1\text{ m s}^{-1}$) of uncertain sign throughout the US [58].

Changes in social, economic and technological factors may also affect the degree to which climate change will impact overall electricity supply adequacy. Electricity load, for instance, is influenced by a host of underlying drivers, including socio-economic factors, residential behaviors, and electricity use for commercial and industrial activities. If these underlying drivers of electricity consumption change, then it is possible that peak load will change as well. Future technological changes—like conductor upgrades and building energy efficiency improvements—represent another major source of uncertainty (SI section 2.6). However, unlike GCM models or conductor cable parameters, technological changes are subject to economic, social and political considerations, and are therefore difficult to quantify. Upgrading existing ACSR cable to heat-resistant ACSS cable offers the potential to offset nearly all climate-attributable ampacity losses. However, it is unclear whether upgrading existing ACSR cables is economically or politically viable. Similarly, a review of the literature reveals that upgrades to building energy efficiency and demand-side management programs have the potential to offset virtually all climate-attributable increases to electricity load (SI section 2.6)—however, it is unclear to what extent these gains will actually be realized. While social and technological changes could have a significant impact on the results of this study, it is difficult to assess what level of change is likely to occur. Thus, rather than

attempting to characterize the effects of social and technological changes as a source of uncertainty, we recommend viewing these changes as a potential mitigation strategy—one that future research should address in detail.

5. Discussion

While climate change may present challenges to peak-period electric power infrastructure, impacts can be offset through carbon mitigation initiatives, re-conducting of congested transmission corridors, building energy efficiency improvements, and new ‘smart-grid’ technologies. Perhaps the most striking result of this study is the degree to which infrastructure impacts are correlated with atmospheric carbon concentration. Impacts to mid-century transmission capacity under the high emissions scenario are about 74% higher than those under the low emissions scenario, while impacts to peak electricity load are about 71% higher. The wide range of impacts between carbon concentration trajectories suggests that policies limiting carbon emissions can go a long way to preventing climate impacts to electricity reliability. Technological improvements also offer the potential to mitigate climate impacts. Upgrades to overhead conductors (such as replacing ACSR cables with more temperature-resistant ACSS cables) have the potential to lessen climate-attributable reductions to transmission capacity. On the demand side, investments in building energy efficiency and demand response programs could offset load increases due to higher air temperatures. Although these changes are difficult to predict in any quantitative capacity, a review of the literature indicates that expansions to demand-side management programs have the potential to reduce future electricity load by 4.0%–27% relative to a ‘business-as-usual’ scenario (SI section 2.6.1). These reductions are comparable to climate-attributable increases in electricity load (4.2%–15%), meaning that investments in building energy efficiency and demand response programs could effectively negate the adverse effects of climate change on the grid.

In addition to conventional best practices, proposed ‘smart grid’ technology may enable the electricity grid to respond more flexibly to climate-constrained conditions (SI section 2.6.2). Smart grid development couples transmission and distribution infrastructure with information and communication technologies to enable advanced power system services [59], including wide-area monitoring systems for large-scale reliability and security assessment, dynamic electricity pricing schemes based on demand response, and the distributed deployment of energy storage, electric vehicle, and renewable power generation resources. Power line temperature and sag monitoring systems can be used with advanced actuator and electricity routing infrastructure to direct

electricity down lines that are less stressed by changing temperature in peak conditions [60]. Moreover, through dynamic ampacity systems, it is possible for thermal limits to better reflect operating conditions by using real-time electrical and environmental data to determine the maximum allowable current for a given power line [60]. This practice enables greater flexibility in how power lines are used to deliver electricity and in planning infrastructure maintenance and upgrades. Smart grid technologies may also help to soften the impact of climate change on electricity load. In future smart grids, distribution systems may monitor and communicate with smart appliances and HVAC systems to control their operation in temperature constrained conditions [61]. For example, to prevent load shedding and infrastructure failures during peak load hours, electric service providers may change the settings on smart A/C units to reduce load within a single home or across multiple buildings within the same circuit. While rising air temperatures may lead to decreased transmission capacity and increased peak loads, impacts to overall electricity reliability can be avoided with the proper mitigation measures in place. Investments in carbon mitigation strategies, demand-side management programs, and smart-grid technologies may lessen or even negate anticipated climate impacts.

The results of this study show that increasing ambient air temperatures may increase electricity demand and decrease transmission ampacity. Additionally, a complementary study on electrical power generation predicts reductions in instantaneous generation capacity in hot summer months for the Western Electricity Coordinating Council (WECC) region [1], which comprises 14 states in the Western US [62]. By mid-century, existing vulnerable summertime generating capacity in the WECC region may be reduced by 1.1%–3.0% in an average year, with proposed capacity (mostly from combustion turbine and solar photovoltaic sources) suffering similar losses [1]. In addition to these losses, increases in ambient air temperature may increase peak per-capita load in the WECC region by as much as 1.7%–14%, while WECC transmission capacity may be reduced by as much as 1.4%–5.6%. This suggests that the joint effect of decreases in generation capacity, decreases in transmission ampacity, and increases in peak load may result in a more constrained electricity grid as ambient temperatures rise. This effect can differ between regions with a summer peak and regions with a winter peak [1, 13]. Regions with a summer peak may have reduced ampacity and increased load (e.g., due to increases in loads from central air conditioners) whereas regions with a winter peak may have increased ampacity and decreased load (e.g., due to decreases in loads from radiative heating). This highlights the need to better understand the impacts of climate change and subsequent rises in ambient temperature on overall electricity system reliability,

both at a general level and for site-specific locations. Currently, some regional electricity supply adequacy assessments do not explicitly account for the effects of climate change [63], meaning that long-term investments in electricity infrastructure may not optimally meet future electricity needs. Site-specific models are needed to explore the combined effects of temperature rise on electricity generation, transmission, distribution, and demand. Further, more work is needed to assess the asynchronous impacts of network congestion and market forces on interconnection-scale electricity supply adequacy. While electricity supply adequacy is adversely affected under all the climate scenarios considered, the results offer several options for alleviating potential impacts, including carbon mitigation initiatives, heat-resistant conductors, building energy efficiency upgrades, and new smart-grid technologies. These measures offer the potential to lessen or even completely offset potential climate impacts, depending on how aggressively they are pursued. While the effects of climate change on electric power infrastructure could be considerable, this study shows that these impacts can be overcome with existing technologies and management techniques, given that anticipatory governance practices can be instituted.

Acknowledgments

This material is based on work supported by the National Science Foundation (grant numbers WSC 1360509, IMEE 1335556, and RIPS 1441352). This work was supported in parts by the USACE Military Programs. Permission was granted by the authority of the USACE Chief of Engineers to publish this material. The views and opinions expressed in this article are those of the individual authors and not those of the U.S. Army or other sponsor organizations.

References

- [1] Bartos MD and Chester MV 2015 Impacts of climate change on electric power supply in the Western United States *Nat. Clim. Change* **5** 748–52
- [2] Van Vliet M T H, Yearsley J R, Ludwig F, Vögele S, Lettenmaier D P and Kabat P 2012 Vulnerability of US and European electricity supply to climate change *Nat. Clim. Change* **2** 676–81
- [3] Sathaye J, Dale L, Larsen P, Fitts G, Koy K, Lewis S and Lucena A 2011 Estimating risk to California Energy Infrastructure from Projected Climate Change, CEC Publication CEC-500-2012-057 (www.energy.ca.gov/2012publications/CEC-500-2012-057/CEC-500-2012-057.pdf)
- [4] Dirks J A *et al* 2015 Impacts of climate change on energy consumption and peak demand in buildings: a detailed regional approach *Energy* **79** 20–32
- [5] Parry M L (ed) 2007 *Climate Change 2007—Impacts, Adaptation and Vulnerability: Working Group II Contribution to the Fourth Assessment Report of the IPCC* vol 4 (Cambridge: Cambridge University Press) (www.ipcc.ch/pdf/assessment-report/ar4/wg2/ar4_wg2_full_report.pdf)
- [6] Harto C B *et al* 2012 Analysis of drought impacts on electricity production in the Western and Texas interconnections of the United States *ANL/EVS/R-11/14*
- [7] Kimmell T A and Veil J A 2009 Impact of drought on US steam electric power plant cooling water intakes and related water resource management issues *DOE/NETL-2009/1364*
- [8] Koch H and Vögele S 2009 Dynamic modelling of water demand, water availability and adaptation strategies for power plants to global change *Ecol. Econ.* **68** 2031–9
- [9] Bartos M and Chester M 2016 Methodology for estimating generating capacity losses in thermoelectric power facilities with recirculating cooling systems under climate change *ASU Digital Repository ASU-SSEBE-CESEM-2016-RPR-003* (<https://repository.asu.edu/items/40430>)
- [10] Dubey S, Sarvaiya J and Seshadri B 2013 Temperature dependent photovoltaic (PV) efficiency and its effect on PV production in the world—a review *Energy Proced.* **33** 311–21
- [11] Janko S, Arnold M and Johnson N 2016 Implications of high-penetration renewables for ratepayers and utilities in the residential solar photovoltaic (PV) market *Appl. Energy* **180** 37–51
- [12] Energy Information Administration 2016 *EIA Form 861: Electric power sales, revenue, and energy efficiency* (<https://eia.gov/electricity/data/eia861/>) (Accessed: September 2016)
- [13] Parkinson S and Djilali N 2015 Robust response to hydro-climatic change in electricity generation planning *Clim. Change* **130** 475–89
- [14] Linkov I *et al* 2014 Changing the resilience paradigm *Nat. Clim. Change* **4** 407–9
- [15] Roeger P E, Collier Z A, Mancillas J, McDonagh J A and Linkov I 2014 Metrics for energy resilience *Energy Policy* **72** 249–56
- [16] PJM Interconnection 2010 *Guide for Determination of Bare Overhead Transmission Conductors* (<http://pjm.com/~media/planning/design-engineering/maac-standards/bare-overhead-transmission-conductor-ratings.ashx>) (Accessed: May 2015)
- [17] PJM Interconnection 2004 *Outdoor Substation Conductor Ratings* (<http://pjm.com/~media/planning/design-engineering/maac-standards/outdoor-substation-conductor-ratings.ashx>) (Accessed: May 2015)
- [18] Rosenthal D H, Gruenspecht H K and Moran E A 1995 Effects of global warming on energy use for space heating and cooling in the United States *Energy J.* **16** 77–96
- [19] Zhou Y, Eom J and Clarke L 2013 The effect of global climate change, population distribution, and climate mitigation on building energy use in the US and China *Clim. Change* **119** 979–92
- [20] Zhou Y *et al* 2014 Modeling the effect of climate change on US state-level buildings energy demands in an integrated assessment framework *Appl. Energy* **113** 1077–88
- [21] Hadley S W, Erickson D J, Hernandez J L, Broniak C T and Blasing T J 2006 Responses of energy use to climate change: a climate modeling study *Geophys. Res. Lett.* **33** L17703
- [22] Mansur E T, Mendelsohn R O and Morrison W 2005 A discrete-continuous choice model of climate change impacts on energy, SSRN Yale SOM Working Paper No. ES-43 (abstract number 738544), submitted to *J. Environ. Manag.*
- [23] McFarland J *et al* 2015 Impacts of rising air temperatures and emissions mitigation on electricity demand and supply in the United States: a multi-model comparison *Clim. Change* **131** 111–25
- [24] Amato A D, Ruth M, Kirshen P and Horwitz J 2005 Regional energy demand responses to climate change: methodology and application to the commonwealth of Massachusetts *Clim. Change* **71** 175–201
- [25] Franco G and Sanstad A H 2007 Climate change and electricity demand in California *Clim. Change* **87** 139–51
- [26] US Energy Information Administration 2011 Fig. of Western U.S. net regional power flows from FERC's Form 714 A quarter of California's electricity comes from outside the state (<http://eia.gov/todayinenergy/detail.cfm?id=4370>) (Accessed: July 2015)

- [27] Allen M, Fernandez S, Fu J and Olama M 2016 Impacts of climate change on sub-regional electricity demand and distribution in the southern United States *Nat. Energy* **1** 16103
- [28] Homeland Security Infrastructure Program 2014 Retail Electric Service Territories Shapefile., United States Department of Homeland Security (CD ROM)
- [29] North American Electric Reliability Corporation 2012 2012 Long-Term Reliability Assessment (<http://nerc.com/news/Headlines%20DL/2012%20Long%20Term%20Reliability%20Assessment.pdf>) (Accessed: June 2015)
- [30] IEEE Standard for Calculating the Current-Temperature Relationship of Bare Overhead Conductors 2013 *IEEE Std 738-2012 (Revision of IEEE Std 738-2006—Incorporates IEEE Std 738-2012 Cor 1-2013)* (doi:10.1109/ieeestd.2013.6692858)
- [31] Homeland Security Infrastructure Program 2014 Electric Transmission Lines Shapefile, United States Department of Homeland Security (CD ROM)
- [32] Southwire Company 2012 *Product Specification—Aluminum Conductor, Steel Reinforced* (<http://southwire.com/ProductCatalog/XTEInterfaceServlet?contentKey=prodcatsheet16>) (Accessed: April 2015)
- [33] Oman Cables Industry 2011 *Overhead Line Conductors* (http://omancables.com/brochure/Overhead_Line_Conductor.pdf) (Accessed: April 2015)
- [34] Nexans Olex New Zealand 2012 *Power Cable Catalogue* Conductor characteristics and product sheets (<http://nexans.co.nz/NewZealand/2013/Power%20Cable%20Catalogue%20Full%20version%202012.pdf>) (Accessed: April 2015)
- [35] House H E and Tuttle P D 1958 Current-carrying capacity of ACSR *Trans. Am. Inst. Elect. Eng.* III **77** 1169–73
- [36] Maurer E P, Wood A W, Adam J C, Lettenmaier D P and Nijssen B 2002 A long-term hydrologically based dataset of land surface fluxes and states for the conterminous United States *J. Clim.* **15** 3237–51
- [37] Shepard D 1984 Computer mapping: the SYMAP interpolation algorithm *Spatial Stat. Mod.* **133**–45
- [38] Widmann M and Bretherton C 2000 Validation of mesoscale precipitation in the NCEP reanalysis using a new gridcell dataset for the northwestern United States *J. Clim.* **13** 1936–50
- [39] Reclamation 2013 Downscaled CMIP3 and CMIP5 Climate Projections: Release of Downscaled CMIP5 Climate Projections, Comparisons with Preceding Information, and Summary of User Needs. Denver, CO: US Department of the Interior, Bureau of Reclamation, Technical Service Center (<http://gdo-dcp.ucllnl.org/>) (Accessed: May 2015)
- [40] California Energy Commission 1999 *High Temperatures and Electricity Demand: An Assessment of Supply Adequacy in California* (Sacramento, CA: the California Energy Commission staff) (www.energy.ca.gov/reports/1999-07-23_HEAT_RPT.PDF)
- [41] Federal Energy Regulatory Commission 2015 *Form No. 714—Annual Electric Balancing Authority Area and Planning Area Report, 1993-2013* (Data set). Retrieved May 2015 from (<http://ferc.gov/docs-filing/forms/form-714/data.asp>)
- [42] US Census Bureau 2015 *Population by census tract, 1990* (Data set) Prepared by Social Explorer (<https://socialexplorer.com/explore/tables>) (Accessed: May 2015)
- [43] US Census Bureau 2015 *Population by census tract, 2000* (Data set) Prepared by Social Explorer (<https://socialexplorer.com/explore/tables>) (Accessed: May 2015)
- [44] US Census Bureau 2015 *Population by census tract, 2010* (Data set) Prepared by Social Explorer (<https://socialexplorer.com/explore/tables>) (Accessed: May 2015)
- [45] US Census Bureau 2015 2014 TIGER/Line Shapefiles—Census Tract Geometries (Data set) (<ftp://ftp2.census.gov/geo/tiger/TIGER2014/>) (Accessed: May 2015)
- [46] US Census Bureau 2015 2000 TIGER/Line Shapefiles—Census Tract Geometries (Data set) (<ftp://ftp2.census.gov/geo/tiger/tiger2k/>) (Accessed: May 2015)
- [47] US Census Bureau 2015 1992 TIGER/Line Shapefiles—Census Tract Geometries (Data set) (<ftp://ftp2.census.gov/geo/tiger/TIGER1992/>) (Accessed: May 2015)
- [48] Cayla J-M, Maizi N and Marchand C 2011 The role of income in energy consumption behaviour: evidence from French households data *Energy Policy* **39** 7874–83
- [49] Wyatt P 2013 A dwelling-level investigation into the physical and socio-economic drivers of domestic energy consumption in England *Energy Policy* **60** 540–9
- [50] Lise W and Van Montfort K 2007 Energy consumption and GDP in Turkey: is there a co-integration relationship? *Energy Econ.* **29** 1166–78
- [51] Sailor D J and Pavlova A A 2003 Air conditioning market saturation and long-term response of residential cooling energy demand to climate change *Energy* **28** 941–51
- [52] Southwire Company 2012 *Product Specification—Aluminum Conductor, Steel Supported, Bare* (<http://southwire.com/ProductCatalog/XTEInterfaceServlet?contentKey=prodcatsheet28>) (Accessed: May 2015)
- [53] Young I R, Zieger S and Babanin A V 2011 Global trends in wind speed and wave height *Science* **332** 451–5
- [54] McVicar T R *et al* 2012 Global review and synthesis of trends in observed terrestrial near-surface wind speeds: implications for evaporation *J. Hydrol.* **416–417** 182–205
- [55] Breslow P B and Sailor D J 2002 Vulnerability of wind power resources to climate change in the continental United States *Renew. Energy* **27** 585–98
- [56] Greene J S, Chatelain M, Morrissey M and Stadler S 2012 Projected future wind speed and wind power density trends over the western US high plains *Atmos. Clim. Sci.* **02** 32–40
- [57] Pryor S C and Barthelmie R J 2011 Assessing climate change impacts on the near-term stability of the wind energy resource over the United States *Proc. Natl Acad. Sci.* **108** 8167–71
- [58] Eichelberger S C J, Nijssen B and Wood A 2008 Climate change effects on wind speed *N. Am. Windpower* **7** 68–72
- [59] Fang X, Misra S, Xue G and Yang D 2012 Smart grid—the new and improved power grid: a survey *IEEE Commun. Surv. Tutorials* **14** 944–80
- [60] Deb A K 2000 *Powerline Ampacity System: Theory, Modeling and Applications* (Boca Raton, FL: CRC)
- [61] Niyato D, Xiao L and Wang P 2011 Machine-to-machine communications for home energy management system in smart grid *IEEE Commun. Mag.* **49** 53–9
- [62] US Department of Energy 2015 *Learn more about interconnections* (<http://energy.gov/oe/services/electricity-policy-coordination-and-implementation/transmission-planning/recovery-act-0>) (Accessed: July 2015)
- [63] North American Electric Reliability Corporation 2015 2015 Long-Term Reliability Assessment (<http://nerc.com/pa/RAPA/ra/Reliability%20Assessments%20DL/2015LTRA%20-%20Final%20Report.pdf>) (Accessed: September 2016)